EUROPHYSICS LETTERS 15 September 2000

Europhys. Lett., **51** (6), pp. 674–678 (2000)

Time-resolved photography of the plasma-plume and ejected particles in laser ablation of polytetrafluoroethylene

N. HUBER, J. GRUBER, N. ARNOLD, J. HEITZ(*) and D. BÄUERLE

Angewandte Physik, Johannes-Kepler-Universität Linz - A-4040 Linz, Austria

(received 12 May 2000; accepted in final form 17 July 2000)

PACS. 79.20.Ds – Laser-beam impact phenomena.
PACS. 61.41.+e – Polymers, elastomers, and plastics.
PACS. 07.68.+m – Photography, photographic instruments and techniques; xerography.

Abstract. – KrF-excimer laser ablation of sintered-powder PTFE targets is successfully used for the deposition of high-quality thin films. The mechanism is based on the high extinction of the pressed-powder targets which causes more efficient dissipation of the incident laser-light energy. As a result, a strongly forward-directed jet of PTFE particles is generated. This jet is investigated by means of a gated ICCD-camera. While the expansion of the visible plume starts with the laser pulse and lasts for about $10\,\mu$s, the particle jet can be observed within a time interval between about $5\,\mu$s and more than $100\,\mu$s after the laser pulse.

Pulsed-laser deposition (PLD) has found increasing interest in thin-film fabrication [1]. With certain systems, the physical properties of PLD films are superior to those produced by conventional techniques such as standard evaporation, electron-beam evaporation, plasma-CVD, etc. An example is the synthesis of polytetrafluoroethylene (PTFE, Teflon) films. Due to the outstanding physical and chemical properties of this material, high-quality films of PTFE are desirable for many applications.

Depending on the experimental conditions and the type of target material employed, the deposited films exhibit strong differences in morphology and electric/dielectric properties. Films deposited from a bulk PTFE target are either amorphous with a high degree of crosslinking, or rough with large particulates incorporated [2, 3]. The electric/dielectric properties of such films are poor. On the other hand, films deposited from sintered-powder pellets are highly crystalline and possess excellent long-time charge stability [4, 5]. These films are superior to those produced by other techniques, and their physical and chemical properties are very similar to regular PTFE [6].

In this letter we investigate the dynamics of laser-induced material removal for two kinds of PTFE targets: polished slabs cut from a PTFE rod and sintered PTFE powder pellets. Both materials (supplied by Goodfellow Corporation) were nominally free of additives. The grain size of the PTFE powder was about 6–9 μm. Its molecular weight was about $5 \cdot 10^4$ to

(*) E-mail: johannes.heitz@jk.uni-linz.ac.at

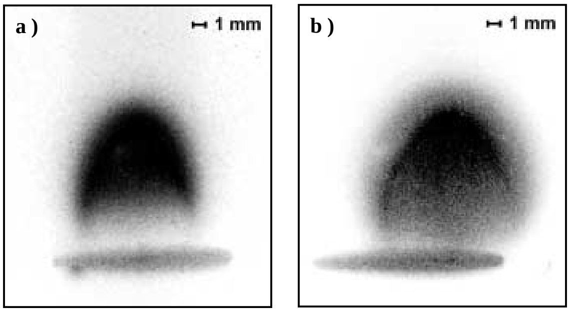

Fig. 1 – Time-resolved ICCD photographs of the expanding vapour/plasma-plume generated by 248 nm KrF-laser radiation at a sintered-powder target (a) and a bulk target (b). The laser pulse energy was $E = 28\,\mathrm{mJ}$, spot diameter $2w = 0.9\,\mathrm{mm}$, and the delay time between the laser pulse and the photograph $t_\mathrm{d} = 1\,\mu\mathrm{s}$. The background atmosphere within the ablation chamber was Ar with a pressure of $p(\mathrm{Ar}) = 0.3\,\mathrm{mbar}$. The lower elliptical disc results from fluorescence light of the target surface.

$4 \cdot 10^5$, compared to $2 \cdot 10^6$ to 10^7 for regular PTFE. The powder was pressed at $3.8 \cdot 10^8\,\mathrm{N/m^2}$ into pellets, which were subsequently sintered at $275\,^\circ\mathrm{C}$ for 24 h.

The experimental setup employed in the investigations was similar to that described in ref. [1]. KrF-excimer-laser (Lambda Physik, LPX 300; pulse duration $\tau_\mathrm{l} \approx 25\,\mathrm{ns}$) radiation was imaged onto the substrate by using a mask together with a 8 : 1 reduction optics. The circular spot on the sample surface had a top-hat profile with a diameter of $2w = 0.9\,\mathrm{mm}$. The target was rotated and the position of the spot was translated via the imaging optics. The background atmosphere within the deposition chamber was high-purity Ar at variable pressures.

The propagation of the vapour/plasma plume was visualised in perpendicular direction by means of an ICCD-camera (Photometrics) equipped with a standard Nikon 50/1.8 objective. This system includes a gateable microchannel plate (MCP) image intensifier. The gate had a variable delay, t_d, with respect to the laser pulse. The gate time was 10 ns.

Pictures of the *visible* plasma plume were recorded for various times, t_d, laser-pulse energies, E, and Ar background pressures, $p(\mathrm{Ar})$. Figures 1a) and b) show photographs of the vapour/plasma plume from a sintered powder and a bulk target, respectively. In both cases, the delay time was $t_\mathrm{d} = 1\,\mu\mathrm{s}$, the laser pulse energy $E = 28\,\mathrm{mJ}$, and the pressure $p(\mathrm{Ar}) = 0.3\,\mathrm{mbar}$. For better visibility, the grey-scale of the picture is inverted, *i.e.*, the darkest areas correspond to the highest emission intensities. The position of the laser spot on the target, and therefore the position of the plume relative to the target, differs in a) and b). The visible plume, which can be detected immediately after the laser pulse, originates from excited ions, atoms and small molecules. The maximum intensity of the emitted light decreases with increasing delay time. It can be observed for several μs, depending on E and $p(\mathrm{Ar})$. For both types of targets, the dynamics of plume expansion is similar, although slight differences can be observed (fig. 1). These differences are probably related to the different surface morphologies, the much stronger optical extinction of the sintered powder target, and the different sizes and velocities of fragments. The plume boundary was defined at 10% of the maximum intensity obtained by the ICCD-camera. This criterion is especially suitable if a clear shock front has formed as in fig. 1a) and b). The boundaries here are outside all visible plume features. Figure 2 shows the normalised length of the plume as a function of the normalised time for the sintered-powder and the bulk-teflon target. In both cases, the expansion dynamics can

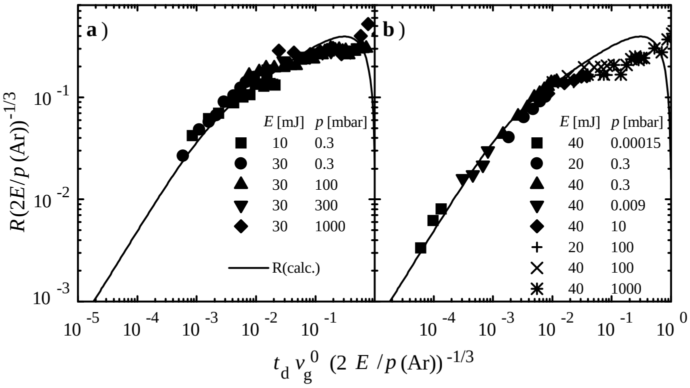

Fig. 2 – Normalised temporal dependence of the distance of the luminous front of the plume from the target during KrF-laser irradiation of a sintered-powder target (a) and a bulk PTFE target (b). The solid curve corresponds to the calculated R derived from the shock-wave model and ν_g^0 is the velocity of sound in the background gas.

be described by the shock-wave model (full curve) [7]. Expansion continues until the pressure within the plume and the external SW decreases and becomes comparable to the pressure of the background gas. The maximum length of the plume is given by [1]

$$R_{\max} \approx k \left(\frac{2E}{p(\mathrm{Ar})} \right)^{1/3}, \tag{1}$$

where k is a constant with values within the range $0 < k \lesssim 1$. k depends on the material properties, the laser wavelength, and pulse duration. For the typical values employed in thin film deposition ($E \approx 15\,\mathrm{mJ}$, $p(\mathrm{Ar}) = 0.3\,\mathrm{mbar}$), we obtain $(R_{\max}/k) \approx 10\,\mathrm{cm}$. This corresponds to the typical target-substrate distances of about 4 cm, which we used during film deposition. The material within the vapour/plasma-plume condenses, at least in part, on the substrate.

In order to observe the "*non-luminous*" material within the plume, an additional series of experiments have been performed. Here, the material ejected from the target was illuminated through an additional glass window of the deposition chamber by means of a conventional photographic flashlight. The flash (duration about $40\,\mu$s) was synchronised with the gate of the ICCD-camera. Except for the delay time the experimental conditions were the same as those employed before. In this case, the pictures are completely different for the two types of targets employed. With the sintered-powder target, a strongly forward-directed jet of particulates is observed, as shown in fig. 3a). This jet appears after a delay time of about $t_\mathrm{d} \approx 5\,\mu$s. It expands to a length of several cm and it can be detected up to times $t_\mathrm{d} \approx 100\,\mu$s. The cross-section of the jet is comparable to the diameter of the laser spot on the target. With the present setup, the size of each pixel of the ICCD-camera corresponds to an area of $45 \times 45\,\mu$m in fig. 3a). From different types of experiments we know that besides large particles which can directly be seen in fig. 3a), also much smaller particles occur during laser ablation of sintered-powder PTFE targets [8]. Thus, in the present experiments we probably detect scattered light not only from large individual particles but also from small particles which are not resolved. The particle jet can be observed after both single-pulse *and* multiple-pulse irradiation of the target. The temporal dependence of the length of the particle jet is plotted in fig. 3b) for different laser-pulse energies and gas pressures.

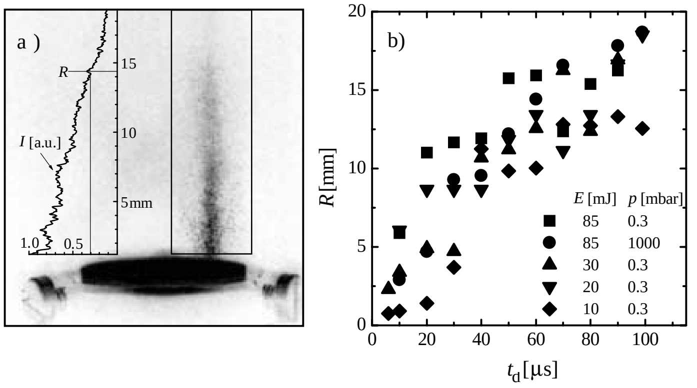

Fig. 3 – Inverted ICCD photographs of flash-illuminated particles ejected from a sintered-powder target ($E = 85\,\text{mJ}$, $p(\text{Ar}) = 1000\,\text{mbar}$, $t_\text{d} = 60\,\mu\text{s}$). The other features are fluorescence light from the target and the screws used to fix the target. For evaluation, the light intensity, I, was horizontally integrated over a frame including the particle jet (a). Temporal dependence of the front of the particle jet, R (defined by $I_\text{front} = 30\% I_\text{max}$) observed with sintered-powder targets (b).

The situation is quite different with bulk targets. Here, *no* particle jet was observed. With single-pulse irradiation only a small number of individual particles leave the target. The situation does not change when the surface is irradiated with a moderate number of laser pulses, $N_\text{l} \lesssim 50$. Condensation of the (small) fragments within the vapour/plasma plume on a substrate yields a very thin amorphous film. With increasing N_l, however, exfoliation of the target and the ejection of large pieces can be seen even by the naked eye. Only a small part of the flakes sticks on the substrate and forms a very rough "film" with poor adhesion. Disruption of bulk PTFE exposed to a large number of KrF-excimer-laser pulses was already reported in ref. [9].

To compare the observed plume and particle distribution to the growth characteristics of the films deposited from pressed-powder targets, we measured the film thickness at various places on the film by means of a masking technique [10]. The local film thickness was fitted by a $\cos^n(\Theta)$-law for the angular distribution of ablated products [1]. The best fit was obtained with $n > 100$. The examination of films deposited with a target-substrate distance of 4 cm by optical microscope indicates that they consist mainly of particles with a diameter between 4 and $60\,\mu\text{m}$. A comparison of the particle size distributions for films deposited at $p(\text{Ar}) = 0.3\,\text{mbar}$ and $p(\text{Ar}) = 100\,\text{mbar}$, respectively, shows a significant reduction of particles with a diameter between 4 and $20\,\mu\text{m}$ in the latter case, probably due to more efficient stopping in the background gas.

In summary, we can say that the experimental investigations presented in this letter confirm earlier speculations on the growth of PTFE films by means of nanosecond KrF-laser radiation [4]. Due to the small absorption coefficient of PTFE at this wavelength ($\alpha(248\,\text{nm}) < 160\,\text{cm}^{-1}$) ablation from bulk targets is very inefficient and results in thin amorphous films consisting of mainly low–molecular-weight fragments. With large numbers of laser pulses ($N_\text{l} > 100$), exfoliation of the target is observed. The deposit then consists of large particulates with low adhesion to the substrate. The situation is quite different with pressed-powder targets. Here, the large extinction coefficient of the material causes efficient dissipation of the incident laser light energy and a strongly forward-directed jet of grains. These grains can be condensed on a preheated substrate. This results in melting and crystallisation of the material and thereby in the formation of relatively smooth ($R_\mathrm{a} < 2\,\mu$m for a film thickness $d = 10\,\mu$m) high-quality thin films.

* * *

This work was supported by the "Fonds zur Förderung der wissenschaftlichen Forschung" under contract P11981-PHY, and the Bundesministerium für Bildung, Wissenschaft und Kultur in Austria.

REFERENCES

[1] Bäuerle D., *Laser Processing and Chemistry*, 3rd edition (Springer, Berlin) 2000.
[2] Jiang W., Norton M. G., Tsung L. and Dickinson J.T., *J. Mater. Res.*, **10** (1995) 1038.
[3] Blanchet G. B., Fincher C. R., Jackson C. L., Shah S. I. and Gardner K. H., *Science*, **262** (1993) 719.
[4] Li S. T., Arenholz E., Heitz J. and Bäuerle D., *Appl. Surf. Sci.*, **125** (1998) 17.
[5] Schwödiauer R., Bauer-Gogonea S., Bauer S., Heitz J., Arenholz E. and Bäuerle D., *Appl. Phys. Lett.*, **73** (1998) 2941.
[6] Schwödiauer R., Heitz J., Arenholz E., Bauer-Gogonea S., Bauer S. and Wirges W., *J. Polym. Sci. B*, **37** (1999) 2115.
[7] Arnold N., Gruber J. and Heitz J., *Appl. Phys. A*, **69** (1999) S87.
[8] Heitz J. and Dickinson J. T., *Appl. Phys. A*, **68** (1999) 515.
[9] Küper S. and Stuke M., *Appl. Phys. Lett.*, **51** (1989) 4.
[10] Huber N., Master thesis, Johannes-Kepler-Universität, Linz (2000).